MOTION OF A RIGID BODY IN A TIDAL FIELD

An Application to Elliptical Galaxies in Clusters

L. CIOTTI[1] and G. GIAMPIERI[2]
[1]*Osservatorio Astronomico di Bologna, via Zamboni 33, I-40126 Bologna, Italy*
[2]*Queen Mary and Westfield College, Astronomy Unit, London E1 4NS, UK*

(Received: 26 August 1997; accepted: 13 January 1998)

Abstract. We investigate the motion, near the equilibrium configurations, of an initially spinless rigid body subject to an external tidal field. Two cases are considered: when the center of mass of the body is at rest at the equilibrium point of the field generated by a generic mass distribution, and when it is placed on a circular orbit subject to a spherically symmetric potential. A complete analysis of the equilibrium configurations is carried out for both cases. First, we derive the conditions for the stable equilibria, and then we analyze the frequencies of oscillations around the equilibrium positions. In view of these results, we consider the problem of alignment of galaxies in clusters. After estimating the period of the oscillations induced on the galaxies by the tidal field of the cluster, we discuss the possible effect of resonances between stellar orbits inside the galaxy and the oscillations of the galaxy as a whole; this may be a mechanism responsible for producing an intracluster stellar population.

Key words: rigid body, analytical methods, elliptical galaxies, cluster of galaxies

1. Introduction

Informations about the structure and evolution of elliptical galaxies (Es) are commonly inferred from their morphology. Roughly speaking, this is justified by the fact that their internal two-body relaxation time is longer than the Hubble time, so that the shape and internal dynamics of such systems probably reflect the conditions present immediately after the end of their formation process (Binney and Tremaine 1987, hereafter BT87). However, a problem with this scenario is that Es in clusters are not isolated objects, being subject to the effects of their environment. Since these effects are acting on time scales shorter than the Hubble time, it is of the utmost importance to be able to isolate them when using the present morphology to infer the conditions at the galaxy formation epoch. In particular, the cluster's tidal field (TF) acts continuously, and affects in general any galaxy in the cluster. Thus, although the TF is not as strong as other interactions (e.g. galaxy–galaxy encounters), its effects can become important on the long term.

A first possibile effect of the TF is a modification of the shape of galaxies belonging to the cluster itself. Ciotti and Dutta (1994, hereafter CD94), using N-body numerical simulations, have shown that this is not the case, since Es behave like rigid bodies in the cluster TF, at variance with disk galaxies (Valluri 1993). Such a conclusion seems

Celestial Mechanics and Dynamical Astronomy **68:** 313–334, 1998.

to be confirmed by observational results, because no systematic differences are found between cluster and field Es (for a review see CD94 and references therein).

A second possible effect on galaxies is their alignment with the cluster major axis, or with the radial direction in the case of a nearly spherical cluster. To this respect, Hawley and Peebles (1975) reported "a possible indication that the galaxies are preferentially aligned along the radius vector to the center of the [Coma] cluster"; this result was confirmed by Thompson (1976). MacGillivray and Dodd (1979a,b) observed an analogous alignment for Es in the cluster centered on NGC439; in this case they found also a number of galaxies with their major axis *perpendicular* to the radial direction of the cluster. The same authors, observing another spherical cluster, found a preferential alignment of Es major axes with the cluster's radial direction. Adams, Strom and Strom (1980) found a general trend for Es to be aligned with the cluster's major axis in 7 very elongated clusters. They also reported "a small but significant number of Es with their major axes perpendicular to the cluster's major axis". Fong, Stevenson and Shanks (1990) found a moderately significant radial alignment of Es, together with a less significant tendency of Es to be oriented *perpendicularly* to this direction. The best evidence for alignment is for the Brightest Cluster Ellipticals: Trevese, Cirimele and Flin (1992) described a "strong alignment of the brightest galaxy major axis with the long axis of the parent cluster".

A third effect strictly related to the previous one is the possible *resonant* interaction between stellar orbits inside the galaxies and the cluster TF: if this is the case then, we can speculate on the possibility of *collisionless evaporation* of stars from galaxies in clusters.

The N-body simulations of prolate Es in radial and circular orbits inside clusters show that an alignment, due to the cluster TF, can in fact be expected (CD94). In this paper, we establish on more firm grounds the analytical discussion of the results of CD94 concerning the alignment. In particular, we discuss the equilibrium positions of a triaxial galaxy at the center of a triaxial cluster, and of a triaxial galaxy in circular orbit inside a spherical cluster, analyzing also the stability of these equilibrium configurations. For small displacements near the stable positions we obtain the oscillation frequencies, which are then compared with the internal orbital periods of the stars. Throughout our discussion (following the N-body results of CD94), a galaxy is described as a rigid body (RB) placed in an external gravitational field. By linearizing the external field, the problem is reduced to that of the integration of the equations of motion for a RB in a tensorial force field, corresponding to the TF. Although this problem is not integrable, one can still determine the equilibrium positions and their stability, along with the proper frequencies of the system.

The paper is organized as follows. In Section 2, we assume that the center of mass of the RB is at rest inside an unspecified external density distribution. In Section 3, we study the more complicate case of a RB on a circular orbit inside an external, spherically symmetric potential. In both cases, we first determine the equilibrium configurations, and then we study their stability. For the stable positions the frequencies are determined analitically. Finally, in Section 4, we discuss the

astronomical application of the previous analysis to the problem of the alignment of galaxies inside galaxy clusters, and of galaxies on circular orbits within spherical clusters. In addition, we compare the mean stellar orbital times inside galaxies with the frequencies induced by the TF, and we consider the possibility of a collisionless evaporation induced by resonances.

2. Body at Rest at the Equilibrium Point of an External Potential

We start discussing the simple case of an initially spinless RB with its center of mass at rest in an equilibrium point of an external potential. We introduce an inertial reference system C, the time-independent density distribution $\rho(\mathbf{x})$ producing the external field $\mathbf{g} = -\nabla\phi(\mathbf{x})$.

Without loss of generality we can assume that the equilibrium point of the potential is at $x = 0$. We also assume that the characteristic dimensions of the RB are much smaller than the typical length-scale over which the external potential changes. Thus, near the equilibrium position

$$\phi(\mathbf{x}) = \phi(0) - \tfrac{1}{2}\langle \mathcal{T}\mathbf{x}, \mathbf{x}\rangle + \mathrm{O}(\|\mathbf{x}\|^3), \tag{1}$$

where the brackets indicates the usual inner product in $\Re^3$ and

$$\mathcal{T}_{ij} \equiv -\left.\frac{\partial^2\phi(\mathbf{x})}{\partial x_i \partial x_j}\right|_{\mathbf{x}=0} \tag{2}$$

is the TF tensor. Note the minus sign in Equations (1)–(2), due to the fact that the TF is defined as the truncation to the first-order of the series expansion of $\mathbf{g}$. We call $\rho_{\mathrm{RB}}(\mathbf{x}; t)$ the density distribution of the RB of total mass M, and we assume that the RB center of mass $\mathbf{R}_{\mathrm{CM}}$ is initially at rest at $\mathbf{x} = 0$. The acceleration of the center of mass is given by

$$M\mathbf{A}_{\mathrm{CM}} = \int \mathbf{g}\rho_{\mathrm{RB}}\,\mathrm{d}^3\mathbf{x} \simeq M\mathbf{g}(\mathbf{R}_{\mathrm{CM}}) + \mathcal{T}(\mathbf{R}_{\mathrm{CM}}) \int (\mathbf{x} - \mathbf{R}_{\mathrm{CM}})\rho_{\mathrm{RB}}\,\mathrm{d}^3\mathbf{x}. \tag{3}$$

It is evident that the last integral vanishes, i.e. the motion of $\mathbf{R}_{\mathrm{CM}}$ is not perturbed in the TF approximation; it is only in higher-order terms of the force expansion that the coupling appears. As a result of the initial conditions imposed, only rotational motions around $\mathbf{x} = 0$ are possible. As usual we indicate with

$$\Im_{ij}(t) = \int (\|\mathbf{x}\|^2\delta_{ij} - x_i x_j)\rho_{\mathrm{RB}}(\mathbf{x}; t)\,\mathrm{d}^3\mathbf{x}, \tag{4}$$

the generic component of the RB inertia tensor $\Im$, as seen from C.

2.1. EQUILIBRIUM CONFIGURATIONS

In order to find the equilibrium configurations of the RB in the TF, we make use of the second cardinal equation of Dynamics, and we search for the vanishing of the torque due to the TF. The tidal torque $\mathbf{N}$ is obtained by the series expansion of its integral definition:

$$N_i = -\epsilon_{ijk} \int x_j \frac{\partial \phi(\mathbf{x})}{\partial x_k} \rho_{\mathrm{RB}}(\mathbf{x}; t)\, \mathrm{d}^3\mathbf{x}, \tag{5}$$

where ϵ_{ijk} is the Levi–Civita tensor (here and in the following, the summation over repeated indices is assumed). Up to now no assumptions have been made about the orientation of the TF with respect to C. Without loss of generality we can assume that $\mathcal{T}$ is in its diagonalized form, so that, using Equation (1) and the antisymmetry of ϵ_{ijk}, Equation (5) can be rewritten as

$$N_i = \sum_{j,k=1}^{3} \frac{\epsilon_{ijk}}{2} \Im_{jk} \Delta T_{jk}, \tag{6}$$

where ΔT is the *antisymmetric* tensor of components $\Delta T_{ij} \equiv T_i - T_j$, and T_i are the three principal values of the TF.

From Equation (6) it is evident that the torque along a particular axis is affected only by the *difference* between the TF components along the two orthogonal directions. It is also obvious that if the external gravitational field is spherically symmetric around $\mathbf{x} = 0$, or if the RB itself is spherically symmetric, then no net momentum acts on the RB, i.e. all its positions are of equilibrium.

We use Equation (6) to find the equilibrium configurations of the RB. Let us define an orthogonal reference system C' with its axes directed along the principal axes of inertia of the RB, and introduce the orthogonal transformation matrix $\mathcal{O}(t)$ between C' and C. In C' the RB is at rest, and its inertia tensor is diagonal, with the three principal components (I_1, I_2, I_3). We consider only a non-degenerate situation (i.e. $I_1 \neq I_2 \neq I_3$ and $T_1 \neq T_2 \neq T_3$). If $\mathcal{O}$ acts on the vectors $\boldsymbol{\xi}$ of C' as $\mathbf{x} = \mathcal{O}\boldsymbol{\xi}$, then the following relation holds:

$$\Im_{jk}(t) = \sum_{\mu=1}^{3} \mathcal{O}_{j\mu}(t) \mathcal{O}_{k\mu}(t) I_\mu. \tag{7}$$

From Equation (6), assuming $\Delta T_{jk} \neq 0$, we conclude that the RB is in equilibrium if and only if $\Im_{jk} = 0$ for $j \neq k$, i.e. if and only if $\Im$ is diagonal. This is true if and only if C and C' are coincident (apart from a renaming of the RB principal axes of inertia). Thus, all the equilibrium positions correspond to the RB inertia axes oriented along the TF principal directions.

2.2. STABILITY

We now consider the Lagrangian $\mathcal{L} = T - U$ associated to our problem. Expanding the external potential as in Equation (1), from Equation (2) and Equation (7) one obtains

$$U = \int \phi(\mathbf{x})\rho_{\mathrm{RB}}(\mathbf{x}; t)\, \mathrm{d}^3\mathbf{x} \simeq M\phi(0) + \pi G\rho(0)\mathrm{Tr}[\Im] + \tfrac{1}{2}\mathcal{O}^2_{i\mu}(t) T_i I_\mu, \qquad (8)$$

where $\mathrm{Tr}[\Im]$ is the trace of the RB inertia tensor, and the property of diagonality of $\mathcal{T}$ in C has been exploited. The first two terms in the r.h.s. of Equation (8) are constant and from now on they will be dropped. Before we proceed, it is necessary to write explicitely the transformation matrix $\mathcal{O}$ between C and C'. Instead of using the usual representation of $\mathcal{O}$ in terms of the Euler angles (i.e. the choice of the 3-1-3 rotations)[1] we adopt the counter-clockwise rotations 1-2-3, namely

$$\mathcal{O} = \mathcal{O}_1(\varphi)\mathcal{O}_2(\vartheta)\mathcal{O}_3(\psi), \qquad (9)$$

with

$$\mathcal{O}_1(\varphi) = \begin{pmatrix} 1 & 0 & 0 \\ 0 & \cos\varphi & -\sin\varphi \\ 0 & \sin\varphi & \cos\varphi \end{pmatrix}, \qquad (10)$$

$$\mathcal{O}_2(\vartheta) = \begin{pmatrix} \cos\vartheta & 0 & \sin\vartheta \\ 0 & 1 & 0 \\ -\sin\vartheta & 0 & \cos\vartheta \end{pmatrix}, \qquad (11)$$

$$\mathcal{O}_3(\psi) = \begin{pmatrix} \cos\psi & -\sin\psi & 0 \\ \sin\psi & \cos\psi & 0 \\ 0 & 0 & 1 \end{pmatrix}. \qquad (12)$$

The angular velocities associated with the rotations around the three inertia axes are $\boldsymbol{\omega}_\phi^{\mathrm{T}} = (\dot\varphi, 0, 0)$, etc, where the suffix 'T' means 'transpose'. By vector composition, the angular velocity of the RB, as seen from C', is:

$$\boldsymbol{\omega} = \boldsymbol{\omega}_\psi + \mathcal{O}_3^{\mathrm{T}}(\psi)[\boldsymbol{\omega}_\vartheta + \mathcal{O}_2^{\mathrm{T}}(\vartheta)\boldsymbol{\omega}_\varphi]. \qquad (13)$$

The kinetic energy of a RB with its center of mass kept fixed is given in C' by

$$\begin{aligned} 2T \;=\; & I_1(\dot\vartheta\sin\psi + \dot\varphi\cos\vartheta\cos\psi)^2 + I_2(\dot\vartheta\cos\psi - \dot\varphi\cos\vartheta\sin\psi)^2 + \\ & + I_3(\dot\psi + \dot\varphi\sin\vartheta)^2. \end{aligned}$$

[1] This choice complicates the treatment due to the indeterminacy of the angles φ and ψ for a null inclination ($\vartheta = 0$).

Similarly, the potential energy U can be expressed as:

$$\begin{aligned} 2U &= (\cos\varphi\cos\psi - \sin\varphi\sin\vartheta\sin\psi)^2\Delta T_{21}\Delta I_{21} + \\ &+ \sin\varphi^2\cos\vartheta^2\Delta T_{21}\Delta I_{31} + \\ &+ (\sin\varphi\cos\psi + \cos\varphi\sin\vartheta\sin\psi)^2\Delta T_{31}\Delta I_{21} + \\ &+ \cos\varphi^2\cos\vartheta^2\Delta T_{31}\Delta I_{31}, \end{aligned} \tag{14}$$

where we have introduced the antisymmetric tensor $\Delta_{ij} = I_i - I_j$, and neglected an additive constant.

As proved in Section 2.1, apart from a renaming of the inertia axes, the equilibrium positions are given by $(\varphi, \vartheta, \psi)_{\text{eq}} = (0, 0, 0)$. The linearized kinetic and potential energy near this point are simply

$$T \simeq \tfrac{1}{2}I_1\dot{\varphi}^2 + \tfrac{1}{2}I_2\dot{\vartheta}^2 + \tfrac{1}{2}I_3\dot{\psi}^2, \tag{15}$$

$$U \simeq -\tfrac{1}{2}\Delta T_{32}\Delta I_{32}\varphi^2 - \tfrac{1}{2}\Delta T_{31}\Delta I_{31}\vartheta^2 - \tfrac{1}{2}\Delta T_{21}\Delta I_{21}\psi^2. \tag{16}$$

Note how both the quadratic forms are already diagonal: this means that, the chosen coordinates (angles) are also the normal coordinates for the problem. The differential equations of the motion are readily obtained:

$$\ddot{\varphi} = \frac{\Delta T_{32}\Delta I_{32}}{I_1}\varphi, \tag{17}$$

$$\ddot{\vartheta} = \frac{\Delta T_{31}\Delta I_{31}}{I_2}\vartheta, \tag{18}$$

$$\ddot{\psi} = \frac{\Delta T_{21}\Delta I_{21}}{I_3}\psi, \tag{19}$$

and their solution is trivial. Note that in the determination of stability positions and relative frequencies, only the *ratios* of the inertia moments matter. Accordingly, in order to simplify our successive discussion in Section 3, we define

$$u \equiv \frac{I_1}{I_3}; \quad v \equiv \frac{I_2}{I_3}. \tag{20}$$

Without loss of generality, let us assume that $T_1 \geqslant T_2 \geqslant T_3$, i.e. that ΔT_{32}, ΔT_{31} and ΔT_{21} are all less or equal to zero. Thus, from Equations (17)–(19), stable motions are possible if and only if $1 > v > u$. In conclusion, a *stable* equilibrium configuration (in the non-degenerate case) is achieved when:

1. The principal axes of the the TF are superimposed with those of the RB;
2. If $T_1 \geqslant T_2 \geqslant T_3$ then $I_1 \leqslant I_2 \leqslant I_3$.

For what concern the behavior of the frequencies, it is obvious that their values increase if we increase the differences between the TF eigenvalues T_i and/or the values of the inertia parameters u, v. In Section 4, the physical meaning of points 1 and 2

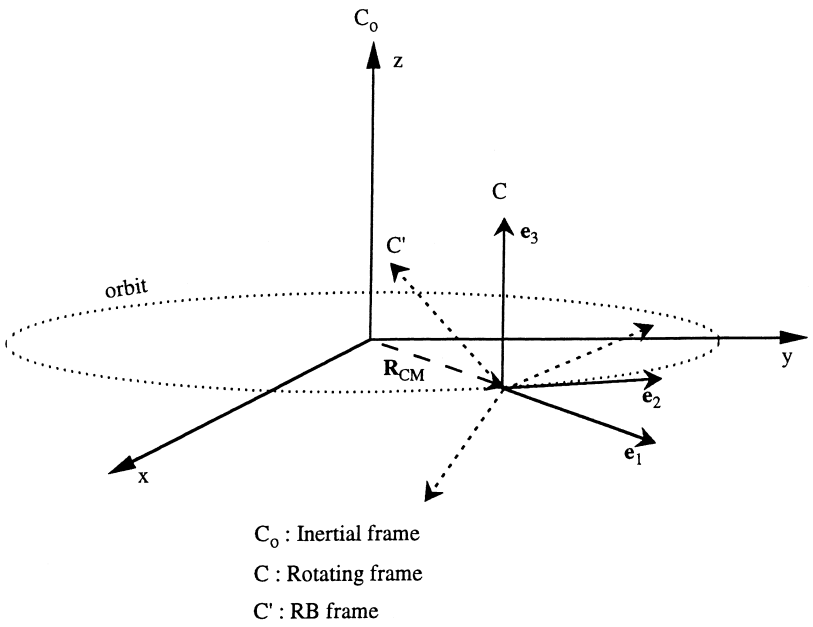

Figure 1. The three reference systems used in the discussion of the RB in circular motion inside a spherical potential.

above will be discussed for our astronomical application, and an explicit calculation of some typical frequencies will be derived for galaxy and clusters models matching observational constraints.

3. Body on a Circular Orbit in a Spherical Potential

In this section, we discuss the case of a triaxial RB on a circular orbit inside a spherically symmetric potential. Note that the assumption that the RB's orbit remains circular is justified by the fact that the external field, truncated at the TF approximation, does not affect the motion of $\mathbf{R}_{\mathrm{CM}}$ (see Section 2).

Without loss of generality, we can assume that the orbit of $\mathbf{R}_{\mathrm{CM}}$ is in the (x, y) plane of the inertial system C_0, the external density is given by $\rho = \rho(r)$ and its associated mass inside the radius r is $M(r)$. The natural frame for our problem (Figure 1) is the *non-inertial* reference system $C = (O; \mathbf{e}_1, \mathbf{e}_2, \mathbf{e}_3)$ with its origin placed at $\mathbf{R}_{\mathrm{CM}}$, $\mathbf{e}_1 = \mathbf{R}_{\mathrm{CM}}/\|\mathbf{R}_{\mathrm{CM}}\|$, and $\mathbf{e}_3$ parallel to the z-axis of C_0. As a consequence C is rotating with the same angular velocity $\boldsymbol{\Omega}$ of $\mathbf{R}_{\mathrm{CM}}$:

$$\boldsymbol{\Omega}^{\mathrm{T}} = (0, 0, \Omega), \qquad \Omega^2 = \left.\frac{GM(r)}{r^3}\right|_{r=R_{\mathrm{CM}}}. \tag{21}$$

We indicate with $\boldsymbol{\xi}$ and $\dot{\boldsymbol{\xi}}$, the generic position and velocity vector in C, respectively related to x and $\dot{x}$ by the usual transformation rules involving the orthogonal transformation matrix C between C_0 and C (see, e.g. Arnold 1978).

3.1. EQUILIBRIUM CONFIGURATIONS

As in the previous case we start discussing the RB equilibrium positions, by means of the second cardinal equation of Dynamics. The relations between the angular momenta and torques in the two systems are given by

$$\mathbf{L}_0 = M\mathbf{R}_{\rm CM} \wedge \mathbf{V}_{\rm CM} + \mathcal{C}(\mathbf{L} + \Im\boldsymbol{\Omega}), \tag{22}$$

and

$$\mathbf{N}_0 = M\mathbf{R}_{\rm CM} \wedge \mathbf{A}_{\rm CM} + \mathcal{C}\mathbf{N}, \tag{23}$$

where $\Im$ is the (time-dependent) RB inertia tensor in C, and

$$\mathbf{L} = \int \boldsymbol{\xi} \wedge \dot{\boldsymbol{\xi}} \rho_{\rm RB}\, {\rm d}^3\boldsymbol{\xi}, \qquad \mathbf{N} = \int \boldsymbol{\xi} \wedge (\mathcal{C}^{\rm T}\mathbf{g}) \rho_{\rm RB}\, {\rm d}^3\boldsymbol{\xi}. \tag{24}$$

From $\dot{\mathbf{L}}_0 = \mathbf{N}_0$ one obtains, upon multiplication by $\mathcal{C}^{\rm T}$:

$$\dot{\mathbf{L}} = \mathbf{N} - \dot{\Im}\boldsymbol{\Omega} - \Im\dot{\boldsymbol{\Omega}} - \boldsymbol{\Omega} \wedge \mathbf{L} - \boldsymbol{\Omega} \wedge \Im\boldsymbol{\Omega}. \tag{25}$$

The equilibrium positions are determined by the request that $\dot{\mathbf{L}} = \mathbf{L} = \dot{\Im} = 0$, along with the condition (verified by hypothesis) that $\dot{\boldsymbol{\Omega}} = 0$. Equation (25) then gives

$$\mathbf{N} - \boldsymbol{\Omega} \wedge \Im\boldsymbol{\Omega} = 0. \tag{26}$$

The first term to be discussed is the tidal torque $\mathbf{N}$. A treatment analogous to that described in Section 2 gives again Equation (6), where now (CD94)

$$\mathcal{T} = -\frac{4\pi G\bar{\rho}}{3} \begin{pmatrix} 3q-2 & 0 & 0 \\ 0 & 1 & 0 \\ 0 & 0 & 1 \end{pmatrix}, \tag{27}$$

having defined

$$q(r) \equiv \frac{\rho(r)}{\bar{\rho}(r)} \leqslant 1^2, \tag{28}$$

where

$$\bar{\rho}(r) \equiv \frac{3M(r)}{4\pi r^3} = \frac{3\Omega^2(r)}{4\pi G}. \tag{29}$$

[2] If ${\rm d}\rho/{\rm d}r \leqslant 0$ then the inequality $q \leqslant 1$ is trivial to prove. If $\rho(r) \propto r^{-\alpha}$ ($\alpha < 3$), then $q = 1 - \alpha/3$. Outside a spherical body $q = 0$.

Note how in this case the TF is degenerate, i.e. two of three TF principal components are equal: $T_2 = T_3$ and so $\Delta T_{23} = 0$; also, $\Delta T_{12} = \Delta T_{13}$.

We can now proceed with the discussion of Equation (26), which gives

$$\Im_{23}\Omega^2 = 0, \tag{30}$$

$$\Im_{13}(\Delta T_{13} + \Omega^2) = 0, \tag{31}$$

$$\Im_{12}\Delta T_{12} = 0. \tag{32}$$

Since from Equations (27) and (28) we get

$$\Delta T_{13} = \Delta T_{12} = 3(1-q)\Omega^2 \geqslant 0, \tag{33}$$

Equations (30)–(32) give the same conditions as in the previous section, namely the equilibrium is achieved when the off-diagonal components of $\Im$ vanish in C, which in this case means that one inertia axis is directed radially, and another is directed along the angular velocity direction. Thus, $\mathbf{\Omega}$ removes the intrinsic degeneracy of the TF.

3.2. STABILITY

We will now linearize $\mathcal{L}$ around the equilibrium points. Let C' be the reference system whose axes are the principal axes of the RB, and $\mathcal{O}$ the transformation matrix between C and C' [see Figure 1 and Equation (9)]. The final expression for the kinetic energy is:

$$T = \frac{MV_{\mathrm{CM}}^2}{2} + \frac{\langle \mathbf{\Omega}' + \boldsymbol{\omega}, I(\mathbf{\Omega}' + \boldsymbol{\omega})\rangle}{2}, \tag{34}$$

where $\boldsymbol{\omega}$, given by Equation (13), is the angular velocity of the RB as seen from C', and $\mathbf{\Omega}' = \mathcal{O}^{\mathrm{T}}\mathbf{\Omega}$.

Obviously, the first term in the r.h.s. of the previous equation is constant, and so can be discarded. Equation (34) contains a term linear in the generalized velocities, a well known consequence of the time dependence of the new coordinate system. With a careful analysis, however, it is easy to prove that this linear component is identically null for a constant $\mathbf{\Omega}$, so that it does not affect the motion. The potential energy remains unaffected by the coordinate change, and its expression is again given by Equation (16). The differential equations associated with the quadratic part of $\mathcal{L}$ are:

$$\ddot{\varphi} = -\frac{\Omega^2\Delta I_{32}}{I_1}\varphi + \frac{\Omega(I_1 + I_2 - I_3)\dot{\vartheta}}{I_1}, \tag{35}$$

$$\ddot{\vartheta} = -\frac{(\Omega^2 + \Delta T_{13})\Delta I_{31}}{I_2}\vartheta - \frac{\Omega(I_1 + I_2 - I_3)\dot{\varphi}}{I_2}, \tag{36}$$

$$\ddot{\psi} = \frac{\Delta T_{21}\Delta I_{21}}{I_3}\psi; \tag{37}$$

note that for $\Omega = 0$ we reobtain Equations (17)–(19) (with $\Delta T_{23} = 0$).

We now analyze the stability of the system described by Equations (35)–(37)[3]. The first result follows directly from Equation (37), from which, by virtue of the assumption $\Delta T_{21} \leqslant 0$, we get the stability condition $I_2 \geqslant I_1$.

Equations (35)–(36), after some standard manipulations, are separated into two linear fourth-order equations with constant coefficients, that are solved setting

$$\varphi(t) \equiv X \exp(\lambda t), \qquad \vartheta(t) \equiv Y \exp(\lambda t). \tag{38}$$

The resulting characteristic equation for λ is biquadratic[4]:

$$\lambda^4 + \alpha\lambda^2 + \beta = 0, \tag{39}$$

where

$$\alpha \equiv \Omega^2 \left[\frac{(u+v-1)^2}{uv} + \frac{1-v}{u} + \frac{(4-3q)(1-u)}{v} \right], \tag{40}$$

$$\beta \equiv \Omega^4 \frac{(4-3q)(1-u)(1-v)}{uv}, \tag{41}$$

and u and v are given in Equation (20). Any solution of Equation (39) is of the form

$$\lambda = \Omega\tilde{\lambda}(u, v; q), \tag{42}$$

where $\tilde{\lambda}$ is a dimensionless function, and the dependence on r is contained in Ω and q. This means that in the determination of stable equilibria only $(u, v; q)$ matter, i.e. the parameter space is three-dimensional. Moreover, for fixed $(u, v; q)$ the frequencies are proportional to Ω, the orbital velocity of $\mathbf{R}_{\rm CM}$ around the center of the external density distribution.

Equation (39) has four solutions: if λ is a root also $-\lambda$ is a root, and so the general solution will contain an exponential increasing term if $\Re\mathrm{e}(\lambda) \neq 0$, making it unstable. The only possibility for a stable equilibrium is then for the four solutions to be purely imaginary, and this is possible if and only if, the two solutions of the associated quadratic equation are real and negative. The reality requires that

$$\Delta \equiv \alpha^2 - 4\beta > 0, \tag{43}$$

and for the negativity it is required that

$$\alpha > 0; \qquad \beta > 0. \tag{44}$$

[3] These linearized equations can also be obtained by expressing Equation (25) in C':

$$I\dot{\boldsymbol{\omega}} = \mathbf{N}' - (\boldsymbol{\Omega}' + \boldsymbol{\omega}) \wedge I(\boldsymbol{\Omega}' + \boldsymbol{\omega}) - I(\boldsymbol{\Omega}' \wedge \boldsymbol{\omega}).$$

Note the identical formal aspect of this system with that discussed in BT87, p. 138 for the stability of Lagrangian points.

[4] The separation introduces two additional integration constants for each variable. These are determined by the requirement that Equations (35)–(36) are satisfied at each instant of time.

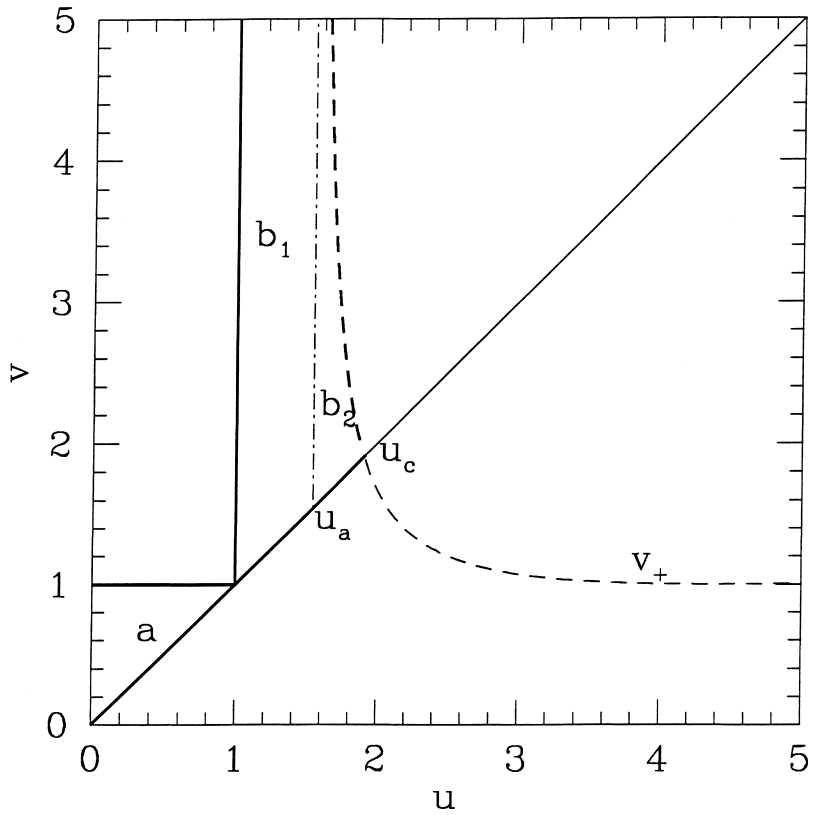

Figure 2. The (u, v) plane with the various critical curves, for $q = 0.9$. In region a the major axis of the RB is directed toward the center of the external potential, the intermediate axis is directed tangentially to the orbit and the minor axis is perpendicular to the orbital plane (Figure 1). In region $b = b_1 \cup b_2$ the major axis of the RB is perpendicular to the orbital plane, the medium axis is directed toward the center, and the short axis is parallel to the orbital velocity.

Note that the conditions (43)–(44) are formally equivalent to the single condition $\alpha > 2\sqrt{\beta}$. The positivity of β is obtained in two different cases:

(a) $u < v < 1$, i.e. $I_3 > I_2 > I_1$.
(b) $1 < u < v$, i.e. $I_2 > I_1 > I_3$.

where the stability of ψ motion ($I_2 > I_1$) has been already assumed.

Case (a) is of easy discussion: in fact, α is a sum of positive quantities, and Δ can be rewritten as a sum of positive quantities as well, independently of the value of $q(r)$. Thus, the motion around the equilibrium position is stable for $I_3 > I_2 > I_1$, for any given density profile of the external density distribution. This corresponds to region (a) in Figure 2.

Case (b) is far more interesting. Its discussion is algebrically cumbersome, but not intrinsically difficult. It can be proved that when $1 < u < v$ the request $\Delta > 0$

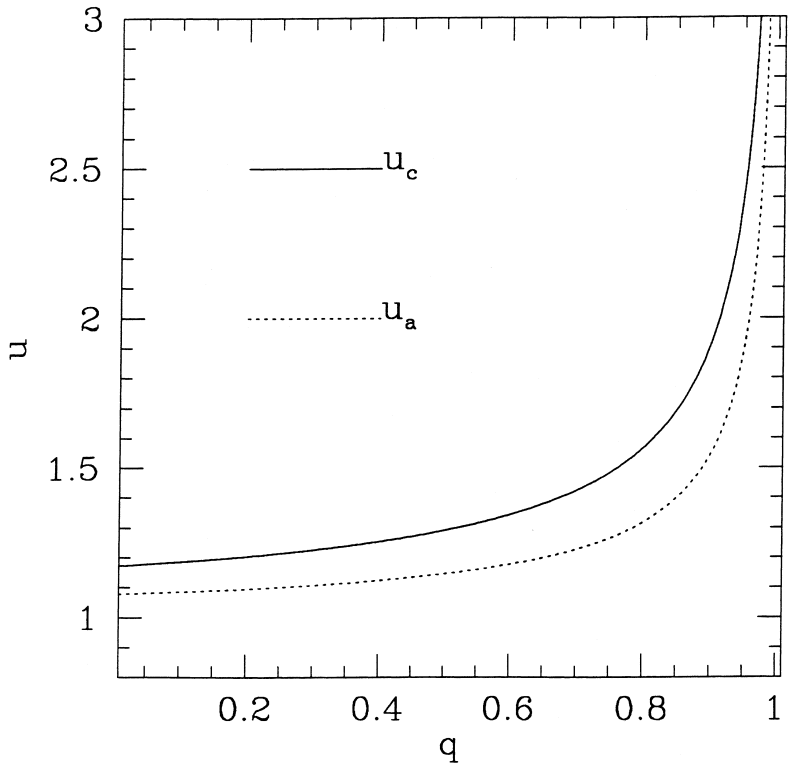

Figure 3. The behavior of u_a and u_c (see Figure 2) as a function of q.

implies $\alpha > 0$, so that the only condition to be studied is $\Delta > 0$. The stability region in the (u, v) plane is plotted in Figure 2 for a specific value of q. Note that the stability region relative to case (b) is made of two qualitatively different parts, separated by a vertical asymptote, located at:

$$u_a(q) = \frac{1}{2} + \frac{1}{2}\sqrt{\frac{4-3q}{3(1-q)}}. \tag{45}$$

In region b_1 ($1 < u < u_a$, see Figure 2) there is no upper bound on I_2/I_3, and $q \to 1 \Rightarrow u_a \to \infty$, i.e. region b_1 expands to all $v > u > 1$. For any finite value of q, there exist another stability region (b_2, see Figure 2) to the right of u_a, whose lower bound is again represented by $v = u$. The upper bound on I_2/I_3 (determined by the condition $\Delta = 0$) is given by

$$v_+ = (u-1)\frac{1 + 9(1-q)u - 6(1-q)u^2 + 6(1-q)u\sqrt{u(u-1)(4-3q)}}{12(1-q)u^2 - 12(1-q)u - 1}, \tag{46}$$

and the point of intersection between $v_+(u)$ and $v = u$ is given by

$$u_c(q) = \frac{1}{2} + \frac{1}{2}\sqrt{\frac{-9q^2 + 6q + 11 + 8\sqrt{4-3q}}{3(1-q)(5+3q)}}. \tag{47}$$

The functions $u_a(q)$ and $u_c(q)$ are plotted in Figure 3. A very important case is obtained for $q = 0$, i.e. in the case of a RB orbiting *outside* a spherical body: in this case the region of equilibrium is very small, since $u_a(0) = 1/2 + 1/\sqrt{3} \simeq 1.08$ and $u_c(0) = 1/2 + 3\sqrt{5}/10 \simeq 1.17$.

3.3. FREQUENCIES

Having found the criteria for stable equilibrium, we now focus our attention on the frequencies of the motions around the $(\varphi, \vartheta, \psi)$ axes. The frequency for the ψ motion is obtained directly from Equation (19) as

$$\frac{2\pi}{P_\psi} = \Omega\sqrt{k(v-u)}; \qquad k \equiv 3(1-q). \tag{48}$$

Its value increases by increasing Ω and/or decreasing q, i.e. by making the external density more concentrated.

The motion around φ and ϑ results from the superposition of two independent oscillations, with frequencies

$$\frac{2\pi}{P_\varphi^\pm} = \frac{2\pi}{P_\vartheta^\pm} = \Omega\sqrt{\frac{1+(\sigma+k)\sigma \pm \sqrt{1+\sigma^2(\tau+k)^2 - 2\sigma(\tau+2k\tau-k)}}{2}}, \tag{49}$$

where

$$\sigma \equiv \frac{1-u}{v}; \qquad \tau \equiv \frac{1-v}{u}.$$

We stress again the presence of the proportionality constant Ω for all frequencies: assuming that the dimensionless factor is of the order of unity, the oscillatory motion around the stable positions is characterized by periods of the order of the RB orbital time.

4. An Astrophysical Application: Galaxies in Clusters

We now apply the previous results to the cases of a triaxial galaxy at the center of a triaxial cluster, and of a triaxial galaxy in circular orbit inside a spherical cluster. We start presenting the galaxy model used.

4.1. THE GALAXY MODEL

We assume that the galaxy density is stratified on homeoidal surfaces labeled by

$$m^2 = \sum_{i=1}^{3} \frac{x_i^2}{\alpha_i^2}, \quad \alpha_1 \geqslant \alpha_2 \geqslant \alpha_3, \tag{50}$$

i.e. $\rho_g = \rho_g(m)$. In the reference system implicitely assumed in Equation (50), all the non-diagonal terms of $\Im$ vanish, and the diagonal terms are given by:

$$I_i = \frac{4\pi}{3}\alpha_1\alpha_2\alpha_3(\alpha_j^2 + \alpha_k^2)h_g; \quad i \neq j \neq k, \tag{51}$$

where the form factor is

$$h_g \equiv \int_0^\infty \rho_g(m)m^4\,\mathrm{d}m. \tag{52}$$

Note that the inertia moments satisfy $I_1 \leqslant I_2 \leqslant I_3$. Note also that in all our results in Sections 2 and 3 only the quantities $u = I_1/I_2$ and $v = I_2/I_3$ appear, and in particular we conclude that for a triaxial homeoidal body the equilibrium positions and the relative frequencies do not depend on the quantity h_g, i.e. they do not depend on the particular density distribution under consideration.

However, a particular density distribution for the galaxy model has to be assumed in order to estimate the characteristic stellar orbital times, and so we adopt an ellipsoidal generalization of the widely used γ-models (Denhen 1993, Tremaine et al. 1994):

$$\rho_g(m) = \frac{M_g}{\alpha_1\alpha_2\alpha_3}\frac{3-\gamma}{4\pi}\frac{1}{m^\gamma(1+m)^{4-\gamma}}, \tag{53}$$

where $0 \leqslant \gamma < 3$. The density in the outer parts goes like m^{-4} independently of γ; for $\gamma = 0$ the models present a flat density *core*. It is straightforward to show that a density stratified on constant m surfaces, when projected on its principal planes, originates a brightness distribution with elliptical isophotes whose ellipticity is the same as that of the corresponding section of the ellipsoid. For example, projecting along x_3 the isophotal axial ratio in the $x_1 - x_2$ plane is α_2/α_1, and the corresponding ellipticity is $\epsilon_{21} = 1 - \alpha_2/\alpha_1$. This property is useful when constructing realistic galaxy models: mean observed values are $\epsilon = 0.2 - 0.4$ (corresponding to E2–E4 galaxies).

For the models described by Equation (53) the mass inside m is given by:

$$M_g(m) = 4\pi\alpha_1\alpha_2\alpha_3\int_0^m \rho_g(t)t^2\,\mathrm{d}t = M_g\frac{m^{3-\gamma}}{(1+m)^{3-\gamma}}, \tag{54}$$

the mean density inside m is

$$\bar{\rho}_g(m) = \frac{M_g}{\alpha_1\alpha_2\alpha_3}\frac{3}{4\pi}\frac{1}{m^\gamma(1+m)^{3-\gamma}}, \tag{55}$$

and an *estimate* of the order of magnitude of the characteristic orbital time of stars inside m is finally obtained as usual as

$$P_{\rm orb}(m) \simeq 4P_{\rm dyn}(m) \equiv \sqrt{\frac{3\pi}{G\bar{\rho}_{\rm g}(m)}}, \tag{56}$$

(BT87, p. 37)[5].

From Equations (55)–(56) one can write

$$P_{\rm orb} = \sqrt{\frac{\alpha_1\alpha_2\alpha_3}{GM_{\rm g}}}\,\tilde{P}_{\rm orb} \simeq 3.0\sqrt{\frac{\alpha_{1,10}^3(1-\epsilon_{21})(1-\epsilon_{31})}{M_{\rm g,11}}}\,\tilde{P}_{\rm orb}(m,\gamma)\times 10^8\,{\rm yr}, \tag{57}$$

where $M_{\rm g,11}$ is the galaxy mass normalized to $10^{11}\ M_\odot$ and $\alpha_{1,10}$ is the galaxy core major axis in 10 kpc. In Figure 4, we plot the dimensionless function $\tilde{P}_{\rm orb}$, for various values of γ.

4.2. TRIAXIAL GALAXIES AT THE CENTER OF TRIAXIAL CLUSTERS

We now focus on the TF produced by a triaxial cluster. We assume that the cluster's density is stratified on homeoidal surfaces $\rho_{\rm c} = \rho_{\rm c}(\ell^2)$, with

$$\ell^2 = \sum_{i=1}^{3}\frac{x_i^2}{a_i^2}; \quad a_1 \geqslant a_2 \geqslant a_3. \tag{58}$$

The associated potential is found using the well-known formulas from potential theory (Kellog 1953; Chandrasekhar 1969, Cap.3; BT87 p. 61). With the aid of the auxiliary function

$$\Psi(\ell^2) \equiv \int_0^{\ell^2}\rho_{\rm c}(t)\,{\rm d}t, \tag{59}$$

the potential can be written as

$$\phi(\mathbf{x}) = -G\pi a_1a_2a_3\int_0^\infty \frac{\Psi(\infty)-\Psi[\ell^2(\tau,\mathbf{x})]}{\Delta(\tau)}\,{\rm d}\tau, \tag{60}$$

where

$$\Delta(\tau) = \sqrt{(a_1^2+\tau)(a_2^2+\tau)(a_3^2+\tau)}, \tag{61}$$

[5] Note that, strictly speaking, the previous formula applies only to the case of a point mass in radial or circular orbit inside a homogeneous, spherically symmetric density distribution. As pointed out by the referee, particular attention should be paid in the case of an incompressible, self-gravitating, prolate spheroid steadily rotating about its axis of symmetry: in fact, in this case the equations of hydrodynamics do not admit solutions (see, e.g. Florides and Spyrou 1993).

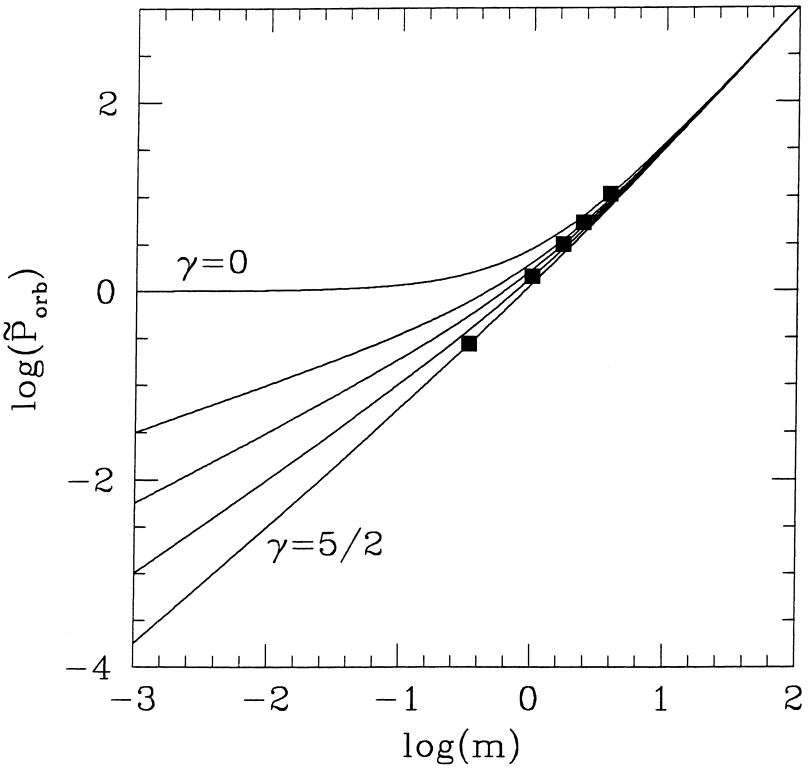

Figure 4. Estimated orbital times as function of m for various γ. The curves from top to bottom correspond, respectively, to γ equal to 0, 1, 1.5, 2, and 2.5. The black diamonds correspond to the half-mass orbital time, i.e. the orbital time calculated at $m_{1/2} = [2^{1/(3-\gamma)} - 1]^{-1}$, the homeoid containing half of the galaxy mass.

and

$$\ell^2(\tau, \mathbf{x}) \equiv \sum_{i=1}^{3} \frac{x_i^2}{a_i^2 + \tau}. \tag{62}$$

The fact that the center of the cluster is an equilibrium point, is trivial to prove and with very simple algebra the following integral expression for the principal components of the TF at the cluster center are found:

$$T_i = -2\pi G \rho_c(0) a_1 a_2 a_3 \int_0^\infty \frac{\mathrm{d}\tau}{(a_i^2 + \tau)\Delta(\tau)}. \tag{63}$$

Note that the particular form of the cluster density distribution does not enter Equation (63), and that if $a_1 \geqslant a_2 \geqslant a_3$ then $T_1 \geqslant T_2 \geqslant T_3$, as assumed in Section 2.2. We can now give the astrophysical interpretation of the results obtained in Section 2.2: the stable equilibrium position of a triaxial galaxy at the center of a triaxial cluster

corresponds geometrically to the three principal axes of the galaxy to be collinear – in the same order – with the principal axes of the cluster density distribution. This configuration reproduces in a natural way the observed "strong alignment of the [brightest] galaxy major axis with the long axis of the parent cluster" (Trevese, Cirimele, Flin 1992), already mentioned in the Introduction.

In order to estimate the oscillatory periods of a galaxy around its equilibrium position, the numerical values of the TF components in a realistic cluster are needed. From Equation (63) one obtains

$$\Delta T_{ij} = -2\pi G\rho_{\rm c}(0)(1-\epsilon_{21})(1-\epsilon_{31})\Delta\tilde{T}_{ij}. \tag{64}$$

The evaluation of the three integrals T_1, T_2 and T_3 involves elliptic functions; in the degenerate case of a rotation ellipsoid these functions can be expressed in terms of elementary functions. The dimensionless quantities $\tilde{T}_i$ are given in Appendix. We obtain $\rho_{\rm c}(0)$ in Equation (64) using the Virial Theorem for the King density distribution (King 1972, BT87 p. 228), from which $\rho_{\rm c}(0) \simeq 9\sigma^2/4\pi G a_1^2$. The time required for a complete oscillation of the galaxy around each of the angular coordinates is then given by

$$\begin{aligned} P_{\rm osc} &= \sqrt{\frac{2\pi}{G\rho_{\rm c}(0)}}\,\tilde{P}_{\rm osc}(u, v, \epsilon_{21}, \epsilon_{31}) \\ &\simeq 7.2\,\frac{a_{1,250}}{\sigma_{1000}}\,\tilde{P}_{\rm osc}(u, v, \epsilon_{21}, \epsilon_{31}) \times 10^8\ {\rm yr}, \end{aligned} \tag{65}$$

where σ_{1000} is the central (one-dimensional) cluster velocity dispersion normalized to 1000 km s^{-1} (a number of order unity for rich clusters), and $a_{1,250}$ is the cluster core major axis normalized to 250 kpc. Following Valluri (1993) and Girardi et al. (1995), we adopt $a_{1,250} = 1$. The explicit expressions for the three $\tilde{P}_{\rm osc}$ can be obtained from Equations (17)–(19). The dimensionality of the parameter space is too large to allow a complete exploration, so we limit ourselves to a specific case. For example, let us assume $a_2/a_1 = 0.8$, $a_3/a_1 = 0.6$, and $\sigma_{1000} = 1$. For the galaxy model, we also adopt $\alpha_2/\alpha_1 = 0.8$ and $\alpha_3/\alpha_1 = 0.6$, corresponding to an E2 and E4 galaxy when the model is projected on the $x_1 - x_2$ and $x_1 - x_3$ planes, respectively. With this choice of parameters, $u = I_1/I_3 = 25/41$ and $v = I_2/I_3 = 34/41$, and the three values of $P_{\rm osc}$ are $(2.7, 1.6, 3.9) \times 10^9$ yrs, for motions around φ, ϑ, ψ, respectively. So, a comparison with the mean stellar orbital times obtained in the previous section (see Figure 4) shows that, in the outer halo of giant Es the stellar orbital times can be of the same order of magnitude as the oscillatory periods of the galaxies themselves. It could be of some interest a numerical investigation of the final fate of these halo stars: in case of escape this is a *collisionless* evaporation. Note that, at variance with the collisional evaporation of globular clusters, in this case no mass segregation is expected, since the effect discussed here is independent of stellar mass. On the contrary, for the bulk of stars in galaxies the orbital times are considerably shorter

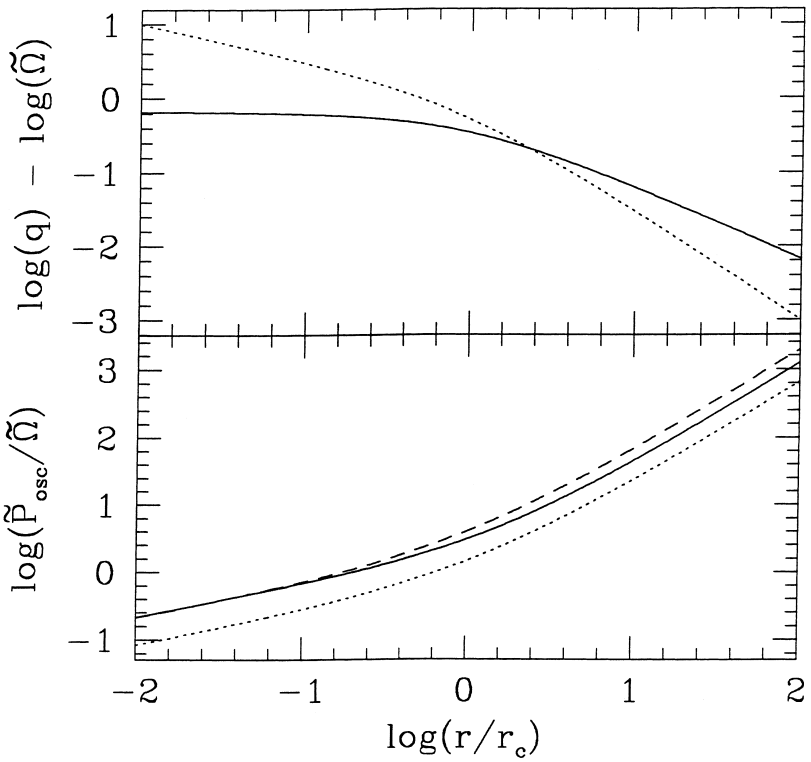

Figure 5. Upper panel: the radial trend of q (solid line) and $\widetilde{\Omega}$ (dotted line) for the Hernquist model. The radius is normalized to the cluster core radius. Lower panel: the radial trend of the three characteristic $\widetilde{P}_{\rm osc}/\widetilde{\Omega}$. The solid line corresponds to the motion around ψ, and the dashed and dotted lines to $P^{-}_{\rm osc}$ and $P^{+}_{\rm osc}$, respectively.

than $P_{\rm osc}$, and this is the reason why in the N-body simulations of CD94 galaxies are found to behave like rigid bodies.

4.3. TRIAXIAL GALAXIES IN CIRCULAR ORBIT IN SPHERICAL CLUSTERS

As shown in Section 3, in this case there are two different equilibrium configurations. The first equilibrium position, with the galaxy's major axis directed toward the galaxy center, reproduces the main observational results already discussed in the Introduction. In the second equilibrium position, the galaxy major axis is *perpendicular* to the orbital plane, as observed for a small number of cases.

In order to analyze the characteristic frequencies around the equilibrium positions in this case, a triaxial galaxy described in Section 4.1 is assumed on circular orbit inside a spherical cluster, described by a Hernquist (1990) density distribution [Equation (53) with $\gamma = 1, \alpha_1 = \alpha_2 = \alpha_3 = r_{\rm c}$]. This assumption about the mass profile follows from the most recent results of cosmological high-resolution collisionless N-body simulations (see, e.g. White 1996, and references therein). From the Virial

Theorem applied to this density law (Hernquist 1990), one finds that $18 r_c \sigma^2 = G M_c$, where σ is the virial one-dimensional velocity dispersion.

The radial trend of $q(r)$ is plotted in Figure 5 (upper panel, solid line): q monotonically decreases moving outwards from the cluster center[6], where $q = 2/3$. In the same figure, we also plot the normalized angular velocity $\widetilde{\Omega} = \Omega/\sqrt{G M_c/r_c^3}$ (dashed line). The equation analogous to Equation (65) is now

$$P_{\rm osc} = \frac{2\pi}{\sqrt{G M_c/r_c^3}} \frac{\widetilde{P}_{\rm osc}(u, v, q)}{\widetilde{\Omega}} \simeq 3.6 \frac{r_{c,250}}{\sigma_{1000}} \frac{\widetilde{P}_{\rm osc}(u, v, q)}{\widetilde{\Omega}} \times 10^8 \,{\rm yr}, \qquad (66)$$

where, for each angle, $\widetilde{P}_{\rm osc}(u, v, q)$ follows from Equations (58)–(59), and is plotted in Figure 5 (lower panel) as a function of r/r_c for the adopted u and v. Note how $P_{\rm osc}$ steadily increases moving outward in the cluster. As a final result there exists a radius approximately of the order of the cluster core where the oscillatory times of galaxies are comparable with their mean stellar orbital times, and so it is possible that some stars will be affected by resonances. The fate of these orbits can be investigated by numerical integration of the equations of motion.

5. Conclusions

In this paper we have presented a discussion of the motion, near the equilibrium configurations, of a rigid body subject to a tidal field. A complete analysis of the equilibrium points when the center of mass of the body is at rest in the field generated by a generic mass distribution, and when it is placed on a circular orbit inside a spherically symmetric potential, was given. The conditions for stable equilibria and the frequencies of oscillations around such positions are analitically derived. As an astrophysical application of the previous results, we have discussed the observed alignment of galaxies in clusters, concluding the numerical investigations presented in CD94. In particular, we have shown that the radially aligned configurations found through N-body simulations by CD94 are indeed equilibrium positions. We have also shown the existence of an equilibrium configuration not found by CD94, i.e. the case of a galaxy in circular orbit in an external spherical potential, whose major axis is perpendicular to the orbital plane; such configurations are observed for a minority of galaxies in real clusters. Moreover, comparing the orbital times of stars inside the model galaxies with the oscillatory times around the equilibrium configurations of the galaxies in the cluster tidal field, we found that for realistic parameters, valid for the majority of the galaxies, the stellar orbital times are much shorter, and so the orbits are adiabatically invariant. This could be an explanation of the result numerically found by CD94 that N-body galaxies behaves in the cluster TF as rigid bodies.

Finally, we have pointed out the possible effect of resonances between stellar orbits in the external parts of the galaxies, and the oscillations frequencies induced on the

[6] For γ-models, $q(r) = (1 - \gamma/3)/(1 + r/r_c)$.

galaxies by the tidal field of the parent cluster. We found that the induced frequencies on galaxies can be of the order of the stellar orbital times in their outer halos and this fact suggests the existence of a possible resonant collisionless evaporation of stars from galaxies in clusters. This mechanism could explain the recently observed population of intracluster stars (see, e.g. Méndez et al. 1997, and references therein).

6. Acknowledgements

LC thanks James Binney and Prasenjit Saha for useful discussions, and the warm hospitality of the Department of Theoretical Physics of Oxford University, where this work was partially carried out. We would like to thank the referee, Prof. Spyrou, for his comments. This work was supported by the EEC contract No. CHRX-CT92-0033 and by the contract ASI-95-RS-152.

Appendix

We start writing explicitely the expressions for the dimensionless functions $\widetilde{T}_i$, defined as $T_i \equiv -2\pi G\rho_c(0)(a_2a_3/a_1^2)\widetilde{T}_i$ [see Equation (63)] in the general triaxial case, defined by $a_1 > a_2 > a_3$.

From Byrd and Friedman (1971, hereafter BF71), defining

$$\theta = \arccos\left(\frac{a_3}{a_1}\right); \qquad k^2 = \frac{1 - a_2^2/a_1^2}{1 - a_3^2/a_1^2}, \tag{67}$$

one obtains

$$\widetilde{T}_1 = \frac{2[F(\theta,k) - E(\theta,k)]}{k^2 \sin^3(\theta)} \tag{68}$$

(BF71, 238.03-310.02),

$$\widetilde{T}_2 = \frac{2[E(\theta,k) - (1-k^2)F(\theta,k) - (a_3/a_2)k^2\sin(\theta)]}{k^2(1-k^2)\sin^3(\theta)}, \tag{69}$$

(BF71, 238.04-318.05), and

$$\widetilde{T}_3 = \frac{2[(a_2/a_3)\sin(\theta) - E(\theta,k)]}{(1-k^2)\sin^3(\theta)}, \tag{70}$$

(BF71, 238.05-316.02), where $F(\theta,k)$ and $E(\theta,k)$ are the Elliptic Integrals of the first and second kind, respectively (see, e.g. BF71, 110.02-100.03).

The first degenerate case is that of a prolate cluster density, i.e. $a_1 > a_2 = a_3$. In this case, the ellipsoidal eccentricity is given by

$$e = \sqrt{1 - \frac{a_2^2}{a_1^2}} \tag{71}$$

and the two different components of the TF are given by:

$$\widetilde{T}_1 = \frac{2}{a_2^2/a_1^2}\left[\frac{1-e^2}{2e^3}\ln\left(\frac{1+e}{1-e}\right) - \frac{1-e^2}{e^2}\right], \tag{72}$$

(Gradshteyn and Ryzhik 1965, Equation 2.248.1; hereafter GR65), and

$$\widetilde{T}_2 = \widetilde{T}_3 = \frac{1}{a_2^2/a_1^2}\left[\frac{1}{e^2} - \frac{1}{2e^3(1-e^2)}\ln\left(\frac{1+e}{1-e}\right)\right], \tag{73}$$

(GR65, 2.248.4). The other degenerate case is the oblate one. We assume now $a_1 = a_2 > a_3$, and so

$$e = \sqrt{1 - \frac{a_3^2}{a_1^2}}. \tag{74}$$

The components of the TF are readily found:

$$\widetilde{T}_1 = \widetilde{T}_2 = \frac{1}{a_3/a_1}\left[\frac{\sqrt{1-e^2}\arcsin(e)}{e^3} - \frac{1-e^2}{e^2}\right], \tag{75}$$

(GR65 2.248.4), and

$$\widetilde{T}_3 = \frac{2}{a_3/a_1}\left[\frac{1}{e^2} - \frac{\sqrt{1-e^2}\arcsin(e)}{e^3}\right], \tag{76}$$

(GR65 2.248.1).

References

Arnold V. I.: 1978, *Mathematical Methods of Classical Mechanics*, Springer-Verlag, New York.
Binney, J. and Tremaine, S.: 1987, *Galactic Dynamics*, Princeton, University Press, Princeton, NJ. (BT87)
Byrd, P. F. and Friedman, M. D.: 1971, *Handbook of Elliptic Integrals for Engineers and Scientists*, Springer-Verlag, New York. (BF71)
Chandrasekhar, S.: 1969, *Ellipsoidal Figures of Equilibrium*, Dover, New York.
Ciotti, L. and Dutta, S. N.: 1994, *MNRAS*, **270**, 390. (CD94)
Dehnen, W.: 1993, *MNRAS*, **265**, 250.

Florides, P. S. and Spyrou, N. K.: 1993, *Ap. J.* **419**, 541.
Fong, R., Stevenson, P. R. F. and Shanks, T.: 1990, *MNRAS*, **242**, 146.
Girardi, M., Biviano, A., Giuricin, G., Mardirossian, F. and Mezzetti, M.: 1995, *Ap. J.* **438**, 527.
Gradshteyn, I. S. and Ryzhik, I. M.: 1965, *Tables of Integrals Series and Products*, Academic Press, London. (GR65)
Hawley, D. L. and Peebles, P. J. E.: 1975, *AJ* **80**, 477.
Kellog, O. D.: 1953, *Foundations of Potential Theory*, Dover, New York.
King, I.: 1972, *Ap. J. L.* **174**, L123.
MacGillivray, H. T. and Dodd, R. J.: 1979a, *MNRAS* **186**, 69.
MacGillivray, H. T. and Dodd, R. J.: 1979b, *MNRAS* **186**, 743.
Méndez, R. H., Guerrero, M. A., Freeman, K. C., Arnaboldi, M., Kudritzki, P., Hopp, U. and Capaccioli, M.: 1997, *Ap. J. L.* **491**, L23.
Rhee, G. and Roos, N.: 1990, *MNRAS* **243**, 629.
Thompson, L. A.: 1976, *Ap. J.* **209**, 22.
Tremaine, S. D., Richstone, D. O., Byun, Y. I., Dressler, A., Faber, S. M., Grillmair, C., Kormendy, J. and Lauer, T. R.: 1994, *AJ*, **107**, 634.
Trevese, D., Cirimele, G. and Flin, P.: 1992, *AJ* **104**, 935.
Valluri, M.: 1993, *Ap. J.* **408**, 57.